Organic & Biomolecular Chemistry

ROYAL SOCIETY OF CHEMISTRY

PAPER

View Article Online
View Journal | View Issue

Cite this: *Org. Biomol. Chem.*, 2021, **19**, 1546

Calix[6]arene-based Brønsted acids for molecular recognition and catalysis†

Gianpiero Cera, * Federica Cester Bonati, Margherita Bazzoni, Andrea Secchi * and Arturo Arduini *

Received 1st December 2020,
Accepted 20th January 2021

DOI: 10.1039/d0ob02393k

rsc.li/obc

We report the synthesis of a versatile trifluoromethylsulfonamide calix[6]arene derivative with Brønsted acid features which can influence both molecular recognition and catalytic application. Indeed, in low polarity media, the trifluoromethyl-containing supramolecular wheel is able to respond to the complexation with charged species as a function of its selective ion-pair recognition. In parallel, the enhanced acidity is the key to promote Michael additions of indoles to nitroalkenes under *pseudo*-physiological reaction conditions (H_2O, 37 °C).

Introduction

Calix[6]arenes represent a fascinating class of macrocycles that has been extensively employed as a platform to construct synthetic receptors for neutral and charged species.[1] In this context, the possibility that this macrocycle could be functionalised regioselectively prompted our research group to introduce a new class of non-palindromic wheels which are able to bind di- and monocationic species in a programmed manner.[2] This finding led to exploiting the reactivity of heteroditopic calix[6]arenes for the synthesis of oriented (pseudo)rotaxanes and stimuli-responsive prototypes of molecular machines.[3] In fact, the threading process that guides the formation of inclusion complexes with viologen salts is highly dominated by hydrogen bonding interactions.[4] Also, in apolar media, phenylureido groups are able to separate the ion pair of the bipyridinium salt, thus dictating the threading of the axle inside the π-rich aromatic cavity. More recently, we demonstrated how aromatic sulfonamide moieties[5] could be employed as binding sites for counterion-dependent molecular recognition of dicationic viologen salts.[6] Remarkably, this class of trisulfonamide calix[6]arenes (TSA) could serve as Brønsted acid catalysts for the Friedel–Crafts-type alkylation reactions in polar protic organic media.[7] These findings are of high importance in the field of calix[6]arene chemistry since, to the best of our knowledge, only hexasulfonated calix[6]arene derivatives display comparable properties (Fig. 1, a).[8] These Brønsted acids, extensively employed in supramolecular chemistry, are able to work as hosting molecules *via* the hydrophobic effect and as catalysts thanks to their acidic sulfonic moieties.[9] In contrast, TSAs exploit their versatile hydrogen-bonding domain to influence both an ion-pair selective formation of pseudorotaxanes and the promotion of catalytic transformations. However, their function is governed by the nature of the substituent on the

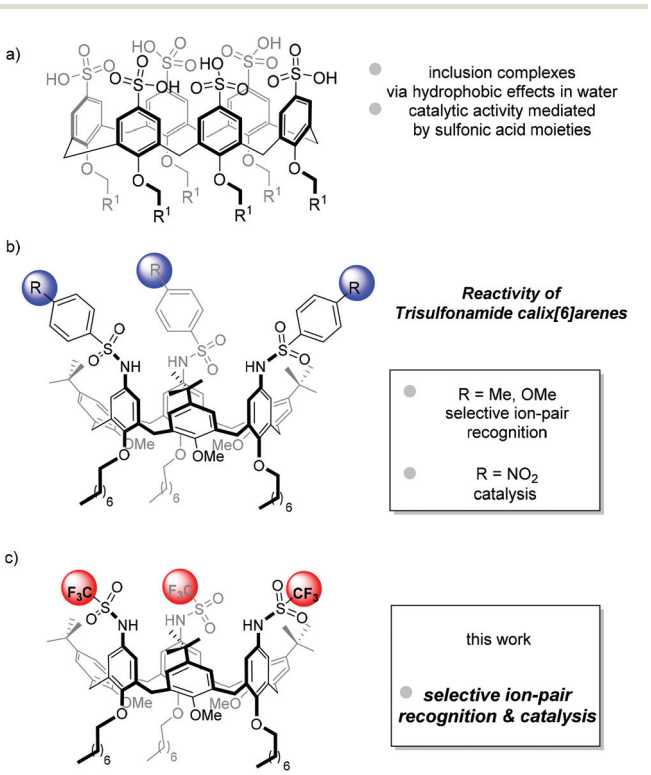

Fig. 1 Comparing the reactivity of hexasulfonated calix[6]arenes with heteroditopic trisulfonamido (TSA) analogues.

Università di Parma, Dipartimento di Scienze Chimiche, della Vita e della Sostenibilità Ambientale, Parco Area delle Scienze 17/A, 43124 Parma, Italy. E-mail: gianpiero.cera@unipr.it, andrea.secchi@unipr.it, arturo.arduini@unipr.it

†Electronic supplementary information (ESI) available. See DOI: 10.1039/d0ob02393k

arene ring. In fact, electron-donating groups are crucial to promoting a highly selective rearrangement of the host in the presence of tight ion-pairs. In contrast, only TSAs, substituted at the *para*-position with three nitro groups, were able to work as effective catalysts (Fig. 1, b).

Prompted by these findings, and inspired by the unique physical and chemical properties of the trifluoromethyl group,[10] we now introduce a new calix[6]arene derivative with the upper ring functionalised with three triflyl-amide moieties (Fig. 1, c). This wheel displays a unified reactivity that allows its function both as a receptor for selective ion-pair recognition and as a highly efficient catalyst for the Michael addition to nitroalkenes.

Results and discussion

At the outset of the investigation, following established protocols,[6] we synthesised a new calix[6]arene derivative **F** from a known trioctyloxy trinitro derivative **TN** (Scheme 1).

Its conformation in solution was subsequently investigated. In apolar solvents, **F** is present as a mixture (2 : 1) of two conformations in a slow exchange at the NMR timescale (see Fig. S2 and 3 in the ESI†). The major one was established to be a typical pseudo *cone* as reflected by its AX system of two doublets with a geminal coupling of ^{2}J = 15.3 Hz of the methylene groups of the calix[6]arene ring. The second, minor one, was attributed to a "distorted" pseudo *cone* conformer. This is characterised by a moderate "down-field" shift (0.5 ppm) of the two methoxy groups in a 2 : 1 ratio analogously to what we previously observed for this class of compounds. Having now at our disposal a family of diversely substituted TSA calix[6]arenes which were previously synthesised in our preliminary studies (Fig. 2, **A**–**E**),[6,7] we decided to investigate the influence of the substitution pattern on their eventual, relative Brønsted acidity.[11] To this end, we compared their interactions with a weak Lewis base such as triethylphosphino oxide (TEPO) in apolar solvents. Indeed, it is known that a rapid formation of a hydrogen bond complex would lead to a single downfield shift of the ^{31}P NMR signal. Taking as a reference the ^{31}P NMR of TEPO (5 mM in C_6D_6), we thus constructed a Gutman–Beckett plot (Fig. 2).[12] Quite expectedly, the *para*-nitro substituted **E** was the most acidic ($\Delta\delta_{PP}$ = 8.7 ppm) along the series of the aromatic sulfonamides that we described in our previous work. However, the newly developed TSA **F**, outcompeted all the other parental TSA calix[6]arenes with a remarkable shift

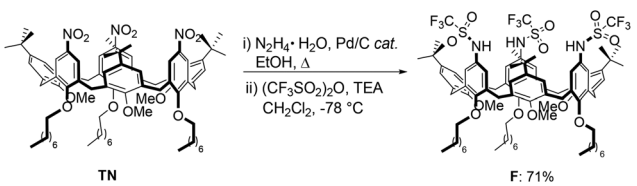

Scheme 1 Synthesis of the trifluoromethyl sulfonamido calix[6]arene TSA **F**.

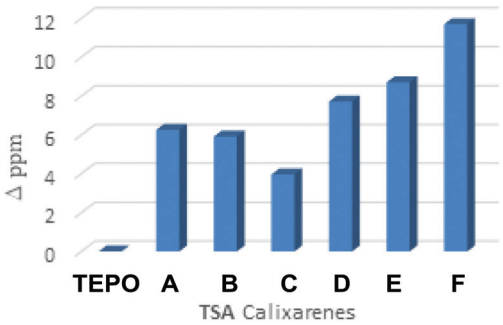

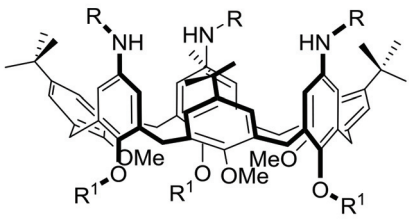

R = 4-$MeC_6H_4SO_2$	R^1 = *n*-Oct	(**A**)[6]
R = 4-$MeC_6H_4SO_2$	R^1 = $(CH_2)_2OEt$	(**B**)[7]
R = 4-$MeOC_6H_4SO_2$	R^1 = *n*-Oct	(**C**)[6]
R = 4-$ClC_6H_4SO_2$	R^1 = *n*-Oct	(**D**)[6]
R = 4-$NO_2C_6H_4SO_2$	R^1 = *n*-Oct	(**E**)[6]
R = CF_3SO_2	R^1 = *n*-Oct	(**F**)

Fig. 2 The Gutmann–Beckett plot showing the influence of TSAs (3 equiv.) on TEPO (1 equiv.) in C_6D_6 as expressed by the variations in the chemical shift of the ^{31}PNMR spectrum when compared to the reference TEPO.

of $\Delta\delta_{PP}$ = 11.7 ppm, highlighting the role of the trifluoromethyl group in increasing the Brønsted acidity of the supramolecular wheel.

It became interesting at this stage to evaluate if this enhanced acidity could deplete the ability of **F** to form inclusion complexes with bipyridinium salts. Hence, we performed spectrophotometric titrations using DOV·2OTs as the guest. The formation of a CT band at 270 nm and an apparent stability constant $\log K_{1:1}$ of 3.5 suggested the formation of a pseudorotaxane complex.[13]

This value, one order of magnitude lower with respect to aromatic TSA pseudorotaxanes, prompted us to compare the apparent stability constants with the corresponding $\Delta\delta_{PP}$ values. We obtained a linear correlation that explains the reduced stability of the complex in terms of enhanced Brønsted acidity of the TSA rather than a depletion of the π-electron-density of the calix[6]arene cavity (Fig. 3).

Subsequently, we equilibrated a solution of **F** in $CDCl_3$ in the presence of a previously employed viologen salt derivative (DOV·2OTs) at 298 K. The ^{1}H-NMR analysis of the resulting yellow mixture highlighted the fairly selective formation of a pseudorotaxane P[**F**(*p*C) ⊃ DOV]2OTs in which the host adopts a *partial cone* conformation (*p*C/C ~ 4 : 1, Fig. 4).

The main features of the ^{1}H-NMR spectrum included a substantial downfield shift (1.5–2 ppm) and the splitting in two

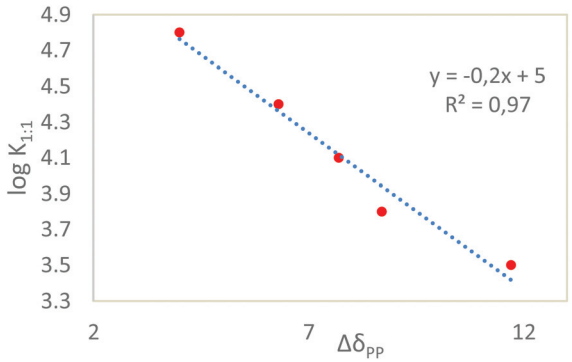

Fig. 3 Log $K_{1:1}$ *vs.* $\Delta\delta_{PP}$ values for P[(**A**, **C**–**F**) ⊃ DOV]2OTs.

signals in a 2 : 1 ratio (£ + $) of the methoxy groups. Furthermore, also in this case, the two doublets of the methylene bridge split into three couples of doublets, one of those (a/a′ couple) suffered a considerable shift of the ^{13}C NMR resonances to δ 35.3 ppm, denotative of an inversion point associated with a methoxy-substituted ring (Fig. S5 and related spectra in the ESI†). Interestingly, the increased Brønsted acidity of **F**, should have led to a drop in the *partial cone vs. cone* selectivity as previously demonstrated for aromatic-substituted TSAs (Table 1, entries 1–4). Nevertheless, complexation of **F** with viologen-based axles, which presents tight ion pairs such as DOV·2OTs, occurs with a selectivity that parallels the features of the electron-rich TSAs **A** and **C** (entry 5). This remarkable effect could be attributed to the limited steric hindrance offered by the trifluoromethyl groups which allow an efficient stabilisation of the *partial cone* conformation. Such a manifold occurs by hydrogen-bonding interactions operated by a tosylate counterion that acts as a bridge between two adjacent trifluoromethylsulfonamide moieties.[6] Encouraged by the features of **F**, we subsequently attempted the complexation using a parental viologen-based axle with two iodides as the weaker coordinating counterions (DOV·2I).

A marked difference was now observed. The NMR analysis showed that **F** is still able to form a pseudorotaxane, but majorly adopting a *cone* conformation (*p*C/C ∼ 1 : 2, entry 5).[13] Hence, in an analogy with the parental TSA **A** (entry 7), calix[6]arene wheel **F** is still able to selectively respond to the complexation with viologen based axles, with a conformational rearrangement dictated by the nature of the ion-pair.[14]

Once having demonstrated that the relative higher acidity of **F** could be still exploited to control the conformation of the newly developed calix[6]arene wheel, we moved our attention to its catalytic application.[15] In particular, one of the most encountered challenges in supramolecular organic chemistry is the development of catalytic methodologies that are able to mimic the high performances offered by biological processes.[16] In this context, enzymes could be considered as the most powerful supramolecular machines due to their ability to promote organic transformations with incredible levels of

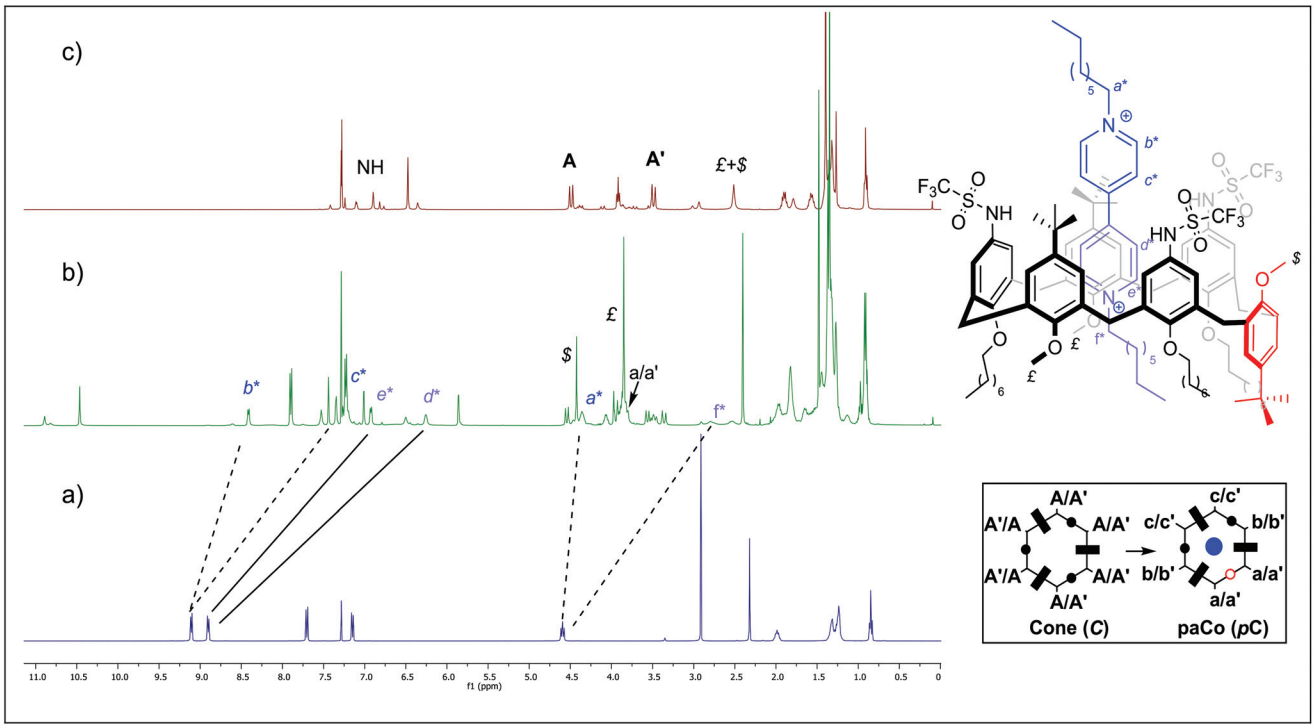

Fig. 4 ^{1}H-NMR spectra (400 MHz, 298 K of (a) DOV·2OTs in CD_3CN, (b) pseudorotaxane P[**F**(*p*C) ⊃ DOV]2OTs in $CDCl_3$, (c) calixarene **F** in $CDCl_3$. Bottom-right: schematic representation of **F** and P[**F**(*p*C) ⊃ DOV]2OTs. The color of the ovals/rectangle indicate the relative position of the phenolic substituent with respect to the plane defined by the bridging methylene groups (hexagon), *i.e.* black upward, white downward. The rectangle identifies the phenolic ring substituted with the octyloxy chains while the circle those with the methoxy groups.

Table 1 Ion-pair selective pseudorotaxane formation using TSA **A**, **C**–**E** and **F**

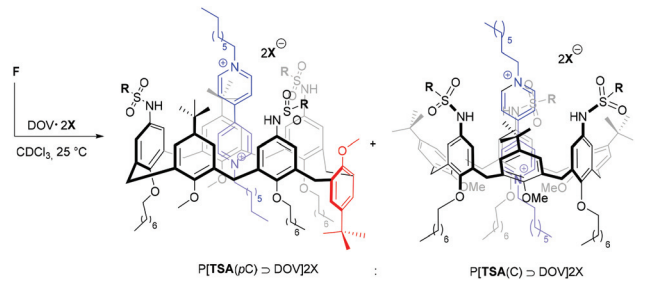

Entry	TSA	X	$\Delta\delta_{PP}$	*p*C : C
1	**A** (R = 4-MeC_6H_4)	OTs	6.3	~5 : 1[a]
2	**C** (R = 4-MeOC_6H_4)	OTs	4.0	~5 : 1[a]
3	**D** (R = 4-ClC_6H_4)	OTs	7.7	~4 : 1[a]
4	**E** (R = 4-$NO_2C_6H_4$)	OTs	8.1	~3 : 1[a]
5	**F** (R = $CF_3C_6H_4$)	OTs	11.7	~4 : 1
6	**F** (R = $CF_3C_6H_4$)	I	11.7	~1 : 2
7	**A** (R = 4-MeC_6H_4)	I	6.3	~1 : 2[a]

[a] See ref. 6.

Table 2 Optimisation of reaction conditions

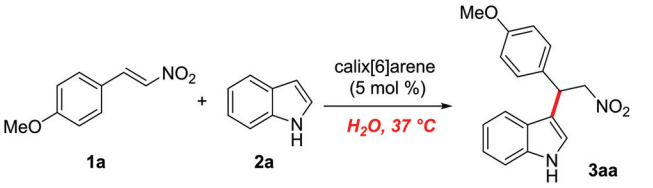

Entry[a]	Calix[6]arene	Conv. [%]	Yields [%]
1	—	45	(42)
2	**A**	75	69
3	**B**	74	71
4	**C**	61	56
5	**D**	75	72
6	**E**	86	82
7	**F**	100	96
8	**G**	69	66
9[b]	**H**	73	70
10[c]	**F**	12	(8)

[a] Reaction conditions: **1a** (0.2 mmol), **2a** (0.6 mmol), calix[6]arene (5 mol%), H_2O (0.5 ml, 0.4 M), 37 °C, 16 h, isolated yields. Yields calculated by ^{1}H-NMR integration using 1,3,5-trimethoxybenzene as an internal standard are shown in brackets. [b] **H** (15 mol%) was employed. [c] Using toluene (0.5 ml, 0.4 M) as the solvent.

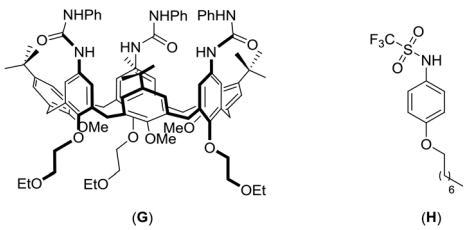

selectivity and efficiency.[17] As a consequence of the ability of TSAs to engage in strong hydrogen bonding interactions with water in the solid state,[7] we thus investigated the possibility of developing a synthetic protocol for a Michael addition of indoles **2** to conjugate alkenes **1**,[18] using water as the safest and environmentally low-impact solvent.

Indeed, after having identified water at 37 °C as the optimal, *quasi*-physiological reaction conditions for the catalysis,[19] we started the screening of the previously synthesised TSAs.

Interestingly, in all the cases under study, "on-water" conditions associated with the use of TSAs (5 mol% loading) led to a notable acceleration of the reactivity.[20] Aromatic sulfonamides **A**–**C** substituted at the *para*-position with EDG groups formed nitroalkane **3aa** with moderate to good yields (entries 2–4, Table 2). Even better results were obtained with TSAs bearing EWG groups such as chlorine (**D**) and the previously employed nitro group (**E**). In fact, **3aa** was isolated with 72% and 82% yields, respectively (entries 5 and 6). To our delight, **F** led to the complete consumption of nitrostyrene **1a** and the corresponding product was delivered with the excellent yield of 96% (entry 7).

Control experiments were subsequently performed. The use of the well-established triphenylureido calix[6]arene **G** led to a marked decrease in the performance of the catalysis (66%, entry 8) due to its intrinsic lower acidity. In parallel, monomeric trifluoromethylsulfonamide **H** followed suit (70%, entry 9). For the sake of comparison, we measured the relative Brønsted acidity of **H** with the Gutmann–Beckett method (see Fig. S4 in the ESI†). Hence, we found a lower shift of the ^{31}P NMR resonance ($\Delta\delta_{PP}$(**H**) = 7.01 *vs.* $\Delta\delta_{PP}$(**F**) = 11.7 ppm), which suggested a cooperative effect of the trifluoromethyl functionalities in TSA **F** as being responsible for the increased acidity of the supramolecular wheel. This effect, in turn, results in an enhanced rate of catalysis. The crucial role of the solvent was finally investigated by performing the reaction in a low-polarity solvent such as toluene, which led to poor conversion of the starting material (entry 10). This effect could be attributed to the presence of a homodromic intra-annular H-bonding domain,[21] which is responsible for the pseudo-*cone* conformation and made the acidic NH bonds of TSA **F** unable to promote a catalytic turnover.

Subsequently, in order to evaluate the applicability of the methodology, we subjected a family of nitroalkenes **1** and indoles **2** to the optimised reaction conditions (Table 3).

Unsubstituted and substituted nitrostyrenes **1b–g** were smoothly converted into products **3ba–ga** with high yields (70–94%). The method proved to be highly performant in the presence of both EDGs and EWGs such as halogens too. An aliphatic nitroalkene **1h** was still applicable to the catalysis leading to **3ha** in slightly diminished yields (86%). Diversely substituted indoles could be employed too. So, indoles bearing EDGs such as an ether or hydroxyl group led to the corresponding products **3bb–bc** in excellent yields (95% and 93%, respectively). Interestingly, while inherently less reactive indoles **2d–f** were found poorly prone to the transformation using **E** (in MeOH at 50 °C), here the use of the newly opti-

Table 3 Scope for the Michael addition

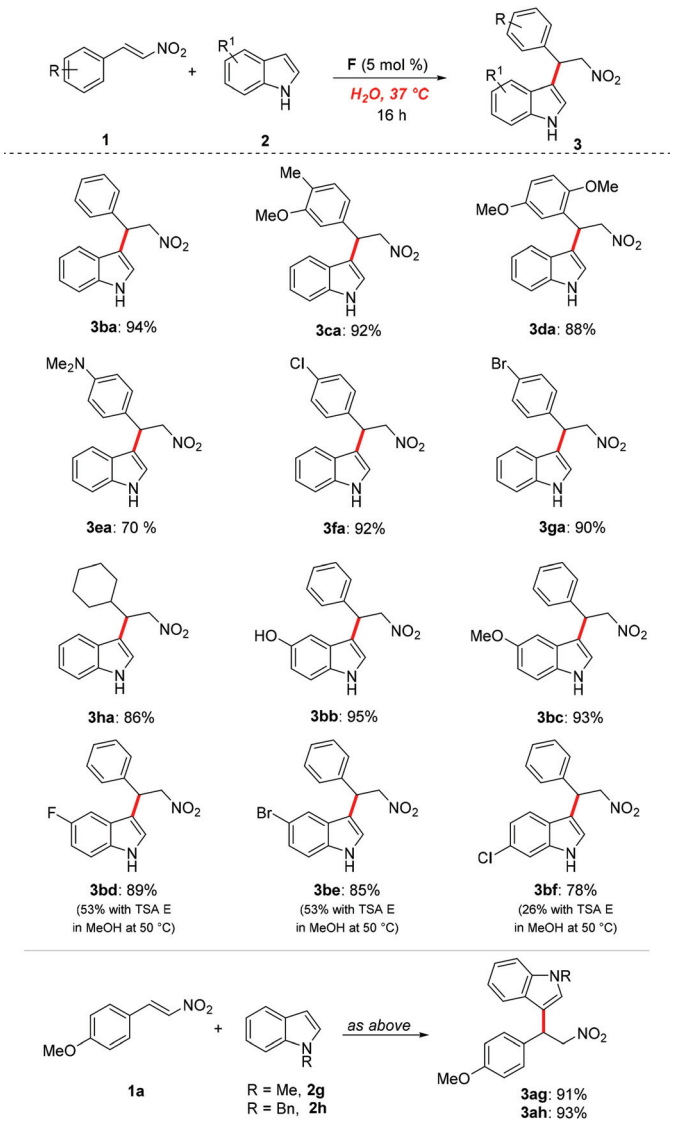

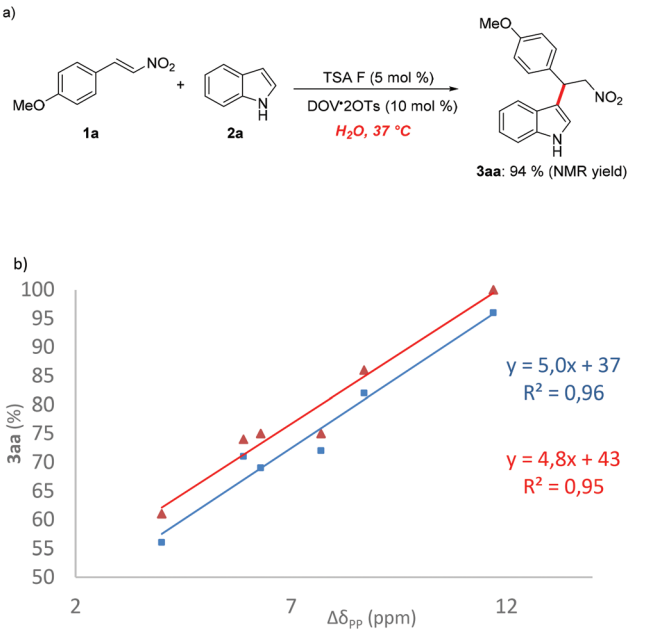

Fig. 5 (a) Model reaction performed in the presence of a competitive guest and (b) outcome of the catalysis with TSAs; NMR conversion (%) in red, isolated yields (%) in blue.

mised protocol was beneficial for the outcome of the catalysis. Hence, differently substituted halogenated indoles led to products **3bd–bf** in good to high yields (78–89%). Finally, the method proved amenable also in the presence of N-protected indole derivatives **2g–h**, with compounds **3ag–ah** transformed in high yields (91–93%, respectively).

The feature of the catalytic methodology led us to interrogate whatever the π-rich aromatic cavity of the calix[6]arene **F** could have a role in promoting the transformation, as for example by threading the nitroalkene reactant.‡ Towards this end, despite the low solubility of **F** in water, we performed the model reaction in the presence of a competitive binder such as dioctyl viologen ditosylate (DOV·2OTs). The reaction yielded the corresponding product **3aa** in comparable yields (94%, NMR yields), excluding the ability of TSAs to catalyse the Michael addition inside the cavity (Fig. 5a, and S7 in the ESI†). We thus tried to correlate both conversions and yields obtained in the optimisation table with the relative Brønsted acidities calculated using the Gutmann–Beckett approach. Interestingly, a linear correlation was observed, suggesting the reactivity of the catalyst to be a function of the enhanced Brønsted acidity of **F** (Fig. 5b).

As for the mechanism, we proposed an outer-sphere manifold in which cooperative trifluorosulfonamide moieties are able to engage in H-bond interactions with the nitro compound, lowering its activation barrier and thus promoting the nucleophilic attack of the indoles.[22] However, the presence of a background reactivity[23] prompts us to not exclude a supramolecular amplification of the acidity of the medium due to a hydrogen-bonding network established between the acidic sulfonamide moieties and water.[24]

Conclusions

We report an exhaustive investigation on the role of Brønsted acidity in the working mode of TSA calix[6]arenes. In particular, we demonstrated how the modified physical and chemical properties, associated with the presence of trifluoromethylsulfonamide moieties, could still be exploited to design ion-pair selective supramolecular receptors, in low polarity solvents. Furthermore, these features allow a dichotomous mani-

‡TSAs are not able to thread nitrostyrenes both in polar (MeOD)[7] and in low polarity solvents ($CDCl_3$, see Fig. S8 in the ESI†). We attempted to investigate the eventual complexation of TSA **F** and **1a** in D_2O by ^{1}H-NMR analysis. However, these reagents are not soluble enough (up to 60 °C) in this medium.

fold for TSAs, promoting a widely applicable catalytic Michael addition to nitrolefines with high levels of efficiency, under *pseudo* physiological reaction conditions. These findings provide a deeper understanding of the reactivity of this novel class of supramolecular wheels and pave the way for a broader application both as receptors and as Brønsted acid catalysts.

Experimental

In a glass tube, **1** (0.2 mmol), **2** (0.6 mmol), and **F** (8.9 mg, 5 mol%) were successively added. Distilled H_2O (0.5 ml, 0.4 M) was added and the reaction mixture placed in a pre-heated oil bath at 37 °C. After 16 h, the reaction mixture was cooled to room temperature and CH_2Cl_2 (10 ml) was added. The mixture was concentrated under reduced pressure and the crude purified by column chromatography on silica gel. All the desired products are known compounds which were characterised by the comparison of their analytical data with those reported in previous literature.

3-(1-(4-Methoxyphenyl)-2-nitroethyl)-1*H*-indole (3aa)[25]

General procedure was followed using **1a** (0.2 mmol, 35.8 mg). Purification by column chromatography (*n*-hex/EtOAc 95 : 5) yielded **3aa** (56.9 mg, 96%) as a white solid. M. p. = 155–157 °C. ^{1}H NMR (400 MHz, CD_2Cl_2) δ = 8.28 (s, 1H), 7.46 (d, J = 7.9 Hz, 1H), 7.42 (d, J = 8.2 Hz, 1H), 7.33–7.28 (m, 2H), 7.25–7.19 (m, 1H), 7.15–7.04 (m, 2H), 6.94–6.87 (m, 2H), 5.20–5.07 (m, 2H), 4.97 (dd, J = 11.7, 8.0 Hz, 1H), 3.81 (s, 3H). ^{13}C NMR (101 MHz, CD_2Cl_2) δ = 159.0, 136.5, 131.4, 128.8, 126.1, 122.5, 121.4, 119.7, 118.8, 114.7, 114.1, 111.4, 79.8, 55.2, 40.8. ESI-MS: m/z $[M + H]^+$ calcd for $C_{17}H_{17}N_2O_3$: 297.12; found: 297.11.

3-(2-Nitro-1-phenylethyl)-1*H*-indole (3ba)[25]

General procedure was followed using **1b** (0.2 mmol, 29.8 mg). Purification by column chromatography (*n*-hex/EtOAc 95 : 5) yielded **3ba** (49.8 mg, 94%) as an off-white solid. M. p. = 98–102 °C. ^{1}H NMR (400 MHz, CD_2Cl_2) δ = 8.30 (s, 1H), 7.48 (d, J = 7.9 Hz, 1H), 7.44–7.35 (m, 4H), 7.34–7.29 (m, 2H), 7.23 (t, J = 7.6 Hz, 1H), 7.14 (d, J = 2.2 Hz, 1H), 7.10 (t, J = 7.6 Hz, 1H), 5.22 (t, J = 7.9 Hz, 1H), 5.14 (dd, J = 12.3, 7.6 Hz, 1H), 5.02 (dd, J = 12.3, 8.4 Hz, 1H). ^{13}C NMR (101 MHz, CD_2Cl_2) δ = 139.6, 136.5, 128.8, 127.8, 127.5, 126.1, 122.6, 121.6, 119.8, 118.7, 114.3, 111.4, 79.6, 41.5. ESI-MS: m/z $[M + H]^+$ calcd for $C_{16}H_{15}N_2O_2$: 267.11; found: 267.14.

3-(1-(3-Methoxy-4-methylphenyl)-2-nitroethyl)-1*H*-indole (3ca)[7]

General procedure was followed using **1c** (0.2 mmol, 38.6 mg). Purification by column chromatography (*n*-hex/EtOAc 95 : 5) yielded **3ca** (56.8 mg, 92%) as a yellow wax. ^{1}H NMR (400 MHz, CD_2Cl_2) δ = 8.22 (s, 1H), 7.46 (dd, J = 8.0, 1.0 Hz, 1H), 7.35 (dt, J = 8.3, 0.8 Hz, 1H), 7.18–7.15 (m, 1H), 7.08–7.02 (m, 3H), 6.82 (d, J = 1.7 Hz, 1H), 6.80 (s, 1H), 5.12 (t, J = 8.0 Hz, 1H), 5.06 (dd, J = 12.3, 8.0 Hz, 1H), 4.95 (dd, J = 12.3, 8.0 Hz, 1H), 3.75 (s, 3H), 2.14 (s, 3H). ^{13}C NMR (150 MHz, CD_2Cl_2) δ = 158.1, 138.4, 136.6, 130.8, 126.2, 125.9, 122.6, 121.6, 119.8, 119.2, 118.8, 114.6, 111.4, 109.8, 79.7, 55.3, 41.6, 15.6. ESI-MS: m/z $[M + H]^+$ calcd for $C_{18}H_{19}N_2O_3$: 311.14; found: 311.19.

3-(1-(2,5-Dimethoxyphenyl)-2-nitroethyl)-1*H*-indole (3da)[26]

General procedure was followed using **1d** (0.2 mmol, 41.8 mg). Purification by column chromatography (*n*-hex/EtOAc 95 : 5) yielded **3da** (57.3 mg, 88%) as a yellow wax. ^{1}H NMR (400 MHz, CD_2Cl_2) δ = 8.29 (s, 1H), 7.52 (d, J = 8.2 Hz, 1H), 7.41 (d, J = 8.2 Hz, 1H), 7.25–7.18 (m, 2H), 7.10 (ddd, J = 7.9, 7.1, 0.9 Hz, 1H), 6.93 (d, J = 8.9 Hz, 1H), 6.81 (dd, J = 8.9, 3.1 Hz, 1H), 6.73 (d, J = 3.1 Hz, 1H), 5.58 (dd, J = 8.7, 7.1 Hz, 1H), 5.15–4.97 (m, 2H), 3.92 (s, 3H), 3.69 (s, 3H). ^{13}C NMR (101 MHz, CD_2Cl_2) δ = 153.6, 151.16, 136.40, 128.60, 126.43, 122.44, 121.97, 119.66, 118.75, 115.70, 113.71, 112.02, 111.76, 111.32, 78.15, 56.00, 55.47, 35.52. ESI-MS: m/z $[M + H]^+$ calcd for $C_{18}H_{19}N_2O_4$: 327.13; found: 327.17.

4-(1-(1*H*-Indol-3-yl)-2-nitroethyl)-*N*,*N*-dimethylaniline (3ea)[25]

General procedure was followed using **1e** (0.2 mmol, 38.4 mg). Purification by column chromatography (*n*-hex/EtOAc 95 : 5) yielded **3ea** (42.9 mg, 66%) as a yellow solid. M. p. = 130–132 °C. ^{1}H NMR (400 MHz, CD_2Cl_2) δ = 8.26 (s, 1H), 7.48 (d, J = 7.2 Hz, 1H), 7.41 (d, J = 8.2 Hz, 1H), 7.23–7.19 (m, 3H), 7.12 (d, J = 2.3 Hz, 1H), 7.10–7.05 (m, 1H), 6.76–6.66 (m, 2H), 5.14–5.05 (m, 2H), 5.00–4.89 (m, 1H), 2.94 (s, 6H). ^{13}C NMR (101 MHz, CD_2Cl_2) δ = 150.0, 136.5, 128.3, 126.7, 126.2, 122.5, 121.3, 119.6, 118.9, 115.1, 112.6, 111.3, 80.0, 40.8, 40.3. ESI-MS: m/z $[M + H]^+$ calcd for $C_{18}H_{20}N_3O_2$: 310.16; found: 310.18.

3-(1-(4-Chlorophenyl)-2-nitroethyl)-1*H*-indole (3fa)[25]

General procedure was followed using **1f** (0.2 mmol, 36.6 mg). Purification by column chromatography (*n*-hex/EtOAc 95 : 5) yielded **3fa** (55.3 mg, 92%) as a yellow solid. M. p. = 108–111 °C. ^{1}H NMR (400 MHz, CD_2Cl_2) δ = 8.32 (s, 1H), 7.48–7.38 (m, 2H), 7.38–7.31 (m, 4H), 7.25 (t, J = 7.6 Hz, 1H), 7.14–7.09 (m, 2H) 5.21 (t, J = 8.2 Hz, 1H), 5.13 (dd, J = 12.3, 8.2 Hz, 1H), 4.99 (dd, J = 12.5, 8.2 Hz, 1H). ^{13}C NMR (101 MHz, CD_2Cl_2) δ = 138.2, 136.5, 133.2, 129.3, 129.0, 125.9, 122.7, 121.6, 119.9, 118.7, 113.8, 111.5, 79.4, 40.9. ESI-MS: m/z $[M + H]^+$ calcd for $C_{16}H_{14}ClN_2O_2$: 301.07; found: 301.06.

3-(1-(4-Bromophenyl)-2-nitroethyl)-1*H*-indole (3ga)[25]

General procedure was followed using **1g** (0.2 mmol, 45.4 mg). Purification by column chromatography (*n*-hex/EtOAc 95 : 5) yielded **3ga** (62.1 mg, 90%) as an off-white solid. M. p. = 120–122 °C. ^{1}H NMR (400 MHz, CD_2Cl_2) δ = 8.32 (s, 1H), 7.54–7.48 (m, 2H), 7.43 (dd, J = 7.5, 3.2 Hz, 2H), 7.31–7.26 (m, 2H), 7.26–7.20 (m, 1H), 7.14–7.07 (m, 2H), 5.25–5.17 (m, 1H), 5.12 (dd, J = 12.3, 7.4 Hz, 1H), 4.98 (dd, J = 12.3, 8.4 Hz, 1H). ^{13}C NMR (101 MHz, CD_2Cl_2) δ = 138.7, 136.5, 131.9, 129.6, 125.9, 122.7, 121.6, 121.3, 119.9, 118.7, 113.7, 111.5, 79.3, 41.0. ESI-MS: m/z $[M + H]^+$ calcd for $C_{16}H_{14}BrN_2O_2$: 345.02; found: 345.03.

3-(1-Cyclohexyl-2-nitroethyl)-1*H*-indole (3ha)[25]

General procedure was followed using **1h** (0.2 mmol, 31.0 mg). Purification by column chromatography (*n*-hex/EtOAc 95 : 5) yielded **3ha** (46.6 mg, 90%) as a yellow wax. ^{1}H NMR (400 MHz, CD_2Cl_2) δ = 8.27 (s, 1H), 7.66 (d, J = 8.1 Hz, 1H), 7.42 (d, J = 8.1 Hz, 1H), 7.29–7.20 (m, 1H), 7.16 (td, J = 7.6, 7.1, 1.0 Hz, 1H), 7.06 (d, J = 2.4 Hz, 1H), 4.89 (dd, J = 11.9, 5.9 Hz, 1H), 4.78 (dd, J = 11.9, 10.0 Hz, 1H), 3.70 (dt, J = 9.9, 6.6 Hz, 1H), 1.98–1.75 (m, 3H), 1.75–1.61 (m, 3H), 1.39–0.97 (m, 5H). ^{13}C NMR (101 MHz, CD_2Cl_2) δ = 136.3, 126.9, 122.4, 122.1, 119.5, 119.0, 113.2, 111.4, 78.7, 41.9, 40.6, 31.2, 30.5, 26.3. ESI-MS: m/z $[M + H]^+$ calcd for $C_{16}H_{21}N_2O_2$: 273.16; found: 273.13.

3-(2-Nitro-1-phenylethyl)-1*H*-indol-5-ol (3bb)[27]

General procedure was followed **1b** (0.2 mmol, 29.8 mg). Purification by column chromatography (*n*-hex/EtOAc 95 : 5) yielded **3bb** (53.6 mg, 95%) as a yellow solid. M. p. = 122–126 °C. ^{1}H NMR (400 MHz, CD_2Cl_2) δ = 8.20 (s, 1H), 7.40–7.35 (m, 4H), 7.35–7.29 (m, 1H), 7.27 (d, J = 8.7 Hz, 1H), 7.11 (d, J = 2.3 Hz, 1H), 6.84 (d, J = 2.3 Hz, 1H), 6.78 (dd, J = 8.7, 2.3 Hz, 1H), 5.17–5.05 (m, 2H), 5.04–4.94 (m, 1H), 4.82 (s, 1H). ^{13}C NMR (101 MHz, CD_2Cl_2) δ = 149.7, 139.5, 131.7, 128.9, 127.7, 127.5, 126.8, 122.6, 113.6, 112.4, 112.1, 103.1, 79.5, 41.5. ESI-MS: m/z $[M + H]^+$ calcd for $C_{16}H_{15}N_2O_3$: 283.11; found: 283.07.

5-Methoxy-3-(2-nitro-1-phenylethyl)-1*H*-indole (3bc)[25]

General procedure was followed using **1b** (0.2 mmol, 29.8 mg). Purification by column chromatography (*n*-hex/EtOAc 95 : 5) yielded **3bc** (55.2 mg, 93%) as a yellow solid. M. p. = 137–140 °C. ^{1}H NMR (400 MHz, CD_2Cl_2) δ = 8.22 (s, 1H), 7.44–7.36 (m, 4H), 7.35–7.26 (m, 2H), 7.09 (d, J = 2.6 Hz, 1H), 6.89 (s, 1H), 6.87 (d, J = 2.4 Hz, 1H), 5.21–5.13 (m, 2H), 5.02 (dd, J = 12.0, 8.3 Hz, 1H), 3.80 (s, 3H). ^{13}C NMR (101 MHz, CD_2Cl_2) δ = 154.2, 139.5, 131.6, 128.9, 127.8, 127.5, 126.5, 122.3, 113.9, 112.5, 112.1, 100.6, 79.5, 55.7, 41.5. ESI-MS: m/z $[M + H]^+$ calcd for $C_{17}H_{17}N_2O_3$: 297.12; found: 297.09.

5-Fluoro-3-(2-nitro-1-phenylethyl)-1*H*-indole (3bd)[27]

General procedure was followed using **1b** (0.2 mmol, 29.8 mg). Purification by column chromatography (*n*-hex/EtOAc 95 : 5) yielded **3bd** (50.7 mg, 89%) as a yellow wax. ^{1}H NMR (400 MHz, CD_2Cl_2) δ = 8.35 (s, 1H), 7.41–7.30 (m, 6H), 7.21 (d, J = 2.1 Hz, 1H), 7.10 (d, J = 9.7 Hz, 1H), 6.98 (td, J = 9.1, 2.1 Hz, 1H), 5.20–5.07 (m, 2H), 5.01 (dd, J = 11.1, 7.0 Hz, 1H). **^{13}C NMR** (101 MHz, CD_2Cl_2) δ = 157.7 (d, $^1J_{C-F}$ = 234 Hz), 139.2, 133.0, 128.9, 127.7, 127.6, 126.5 (d, $^5J_{C-F}$ = 10 Hz), 123.3, 114.4 (d, $^6J_{C-F}$ = 5 Hz), 112.2 (d, $^4J_{C-F}$ = 11 Hz) 110.9 (d, $^2J_{C-F}$ = 26 Hz), 103.7 (d, $^3J_{C-F}$ = 24 Hz), 79.5, 41.4. ESI-MS: m/z $[M + H]^+$ calcd for $C_{16}H_{14}FN_2O_2$: 285.10; found: 285.11.

5-Bromo-3-(2-nitro-1-phenylethyl)-1*H*-indole (3be)[25]

General procedure was followed using **1b** (0.2 mmol, 29.8 mg). Purification by column chromatography (*n*-hex/EtOAc 95 : 5) yielded **3be** (58.6 mg, 85%) as a white solid. M. p. = 134–137 °C. ^{1}H NMR (400 MHz, CD_2Cl_2) δ = 8.40 (s, 1H), 7.60 (s, 1H), 7.43–7.28 (m, 7H), 7.17 (d, J = 1.8 Hz, 1H), 5.22–5.05 (m, 2H), 5.00 (dd, J = 12.2, 8.0 Hz, 1H). ^{13}C NMR (101 MHz, CD_2Cl_2) δ = 139.1, 135.1, 128.9, 127.9, 127.7, 127.6, 125.4, 122.9, 121.3, 114.0, 113.0, 112.9, 79.5, 41.3. ESI-MS: m/z $[M + H]^+$ calcd for $C_{16}H_{14}BrN_2O_2$: 345.03; found: 345.06.

6-Chloro-3-(2-nitro-1-phenylethyl)-1*H*-indole (3bf)[28]

General procedure was followed using **1b** (0.2 mmol, 29.8 mg). Purification by column chromatography (*n*-hex/EtOAc 95 : 5) yielded **3bf** (46.4 mg, 77%) as a yellow wax. ^{1}H NMR (400 MHz, CD_2Cl_2) δ = 8.33 (s, 1H), 7.44–7.41 (m, 1H), 7.40–7.35 (m, 5H), 7.35–7.29 (m, 1H), 7.15 (d, J = 1.8 Hz, 1H), 7.06 (dd, J = 8.6, 1.8 Hz, 1H), 5.19 (t, J = 7.9 Hz, 1H), 5.11 (dd, J = 12.3, 7.8 Hz, 1H), 5.00 (dd, J = 12.3, 8.1 Hz, 1H). ^{13}C NMR (101 MHz, CD_2Cl_2) δ = 139.2, 136.8, 128.9, 128.4, 127.7, 127.6, 124.81, 122.3, 120.4, 119.8, 114.6, 111.3, 79.5, 41.4. ESI-MS: m/z $[M + H]^+$ calcd for $C_{16}H_{14}ClN_2O_2$: 301.07; found: 301.03.

3-(1-(4-Methoxyphenyl)-2-nitroethyl)-1-methyl-1*H*-indole (3ag)[29]

General procedure was followed using **1a** (0.2 mmol, 35.8 mg). Purification by column chromatography (*n*-hex/EtOAc 95 : 5) yielded **3ag** (56.2 mg, 91%) as a whitish oil. ^{1}H NMR (400 MHz, CD_2Cl_2) δ = 7.47 (d, J = 7.9 Hz, 1H), 7.35 (d, J = 8.2 Hz, 1H), 7.32–7.19 (m, 3H), 7.09 (t, J = 7.4 Hz, 1H), 6.96 (s, 1H), 6.90 (d, J = 7.2 Hz, 2H), 5.20–5.06 (m, 2H), 5.02–4.90 (m, 1H), 3.81 (s, 3H), 3.78 (s, 3H). ^{13}C NMR (101 MHz, CD_2Cl_2) δ = 159.0, 137.3, 131.6, 128.8, 126.5, 126.1, 122.1, 119.2, 118.8, 114.1, 113.0, 109.5, 79.8, 55.2, 40.8, 32.7. ESI-MS: m/z $[M + H]^+$ calcd for $C_{18}H_{19}N_2O_2$: 311.14; found: 311.17.

1-Benzyl-3-(1-(4-methoxyphenyl)-2-nitroethyl)-1*H*-indole (3ah)[29]

General procedure was followed using **1a** (0.2 mmol, 35.8 mg). Purification by column chromatography (*n*-hex/EtOAc 95 : 5) yielded **3ah** (71.6 mg, 93%) as a whitish oil. ^{1}H NMR (400 MHz, CD_2Cl_2) δ = 7.49 (d, J = 7.9 Hz, 1H), 7.39–7.29 (m, 6H), 7.21 (d, J = 7.7 Hz, 1H), 7.15 (d, J = 7.2 Hz, 2H), 7.10 (d, J = 7.8 Hz, 2H), 6.92 (d, J = 7.3 Hz, 2H), 5.35 (s, 2H), 5.19 (t, J = 7.8 Hz, 1H), 5.16–5.07 (m, 1H), 5.02–4.93 (m, 1H), 3.82 (s, 3H). ^{13}C NMR (101 MHz, CD_2Cl_2) δ = 159.0, 137.6, 136.9, 131.5, 128.8, 128.7, 127.6, 126.9, 126.7, 125.6, 122.3, 119.5, 119.1, 114.2, 113.8, 110.0, 79.9, 55.2, 50.1, 40.9. ESI-MS: m/z $[M + H]^+$ calcd for $C_{24}H_{23}N_2O_3$: 387.17; found: 387.19.

Conflicts of interest

There are no conflicts to declare.

Acknowledgements

The authors thank Centro Interdipartimentale di Misure of the University of Parma for NMR measurement and B.Sc. student Nicholas Grassi for experimental support. Chiesi Farmaceutici SpA is acknowledged for the support for the D8 Venture. This

work was supported by the Italian MIUR (PRIN 20173L7W8 K). This work was carried out within the COMP-HUB Initiative, funded by the "Departments of Excellence" program of the Italian Ministry of Education, University and Research (MIUR, 2018–2020).

Notes and references

1 (*a*) V. Balzani, A. Credi and M. Venturi, *Molecular Devices and Machines: Concepts and Perspectives for the Nanoworld*, Wiley-VCH, Weinheim, 2nd edn, 2008; (*b*) V. Balzani, A. Credi and M. Venturi, *Molecular Devices and Machines–A Journey into the Nano World*, Wiley-VCH, Weinheim, 2003; (*c*) V. Balzani, A. Credi, F. M. Raymo and J. F. Stoddart, *Angew. Chem., Int. Ed.*, 2000, **39**, 3348.

2 (*a*) A. Arduini, F. Ciesa, M. Fragassi, A. Pochini and A. Secchi, *Angew. Chem., Int. Ed.*, 2005, **44**, 282; (*b*) A. Arduini, R. Ferdani, A. Pochini, A. Secchi and F. Ugozzoli, *Angew. Chem., Int. Ed.*, 2000, **39**, 3453.

3 (*a*) G. Orlandini, L. Casimiro, M. Bazzoni, B. Cogliati, A. Credi, M. Lucarini, S. Silvi, A. Arduini and A. Secchi, *Org. Chem. Front.*, 2020, **7**, 648; (*b*) M. Bazzoni, F. Terenziani, F. A. Secchi, G. Cera, I. Jabin, G. De Leener, M. Luhmer and A. Arduini, *Chem. – Eur. J.*, 2020, **26**, 3022; (*c*) M. Bazzoni, V. Zanichelli, L. Casimiro, C. Massera, A. Credi, A. Secchi, S. Silvi and A. Arduini, *Eur. J. Org. Chem.*, 2019, **2019**, 3513; (*d*) V. Zanichelli, M. Bazzoni, A. Arduini, P. Franchi, M. Lucarini, G. Ragazzon, A. Secchi and S. Silvi, *Chem. – Eur. J.*, 2018, **24**, 12370; (*e*) V. Zanichelli, G. Ragazzon, G. Orlandini, M. Venturi, A. Credi, S. Silvi, M. Bazzoni, A. Arduini and A. Secchi, *Org. Biomol. Chem.*, 2017, **15**, 6753.

4 A. Credi, S. Dumas, S. Silvi, M. Venturi, A. Arduini, A. Pochini and A. Secchi, *J. Org. Chem.*, 2004, **69**, 5881.

5 Selected examples of sulfonamide-based supramolecular receptors, see: (*a*) Y. S. Park, Y. Kim and K. Paek, *Org. Lett.*, 2019, **21**, 8300; (*b*) S. Taghvaei-Ganjali, M. Rasouli-Saniabadi and M. S. Mirmoeini, *J. Inclusion Phenom. Macrocyclic Chem.*, 2015, **83**, 45; (*c*) A. Arduini, E. Brindani, G. Giorgi, A. Pochini and A. Secchi, *J. Org. Chem.*, 2002, **67**, 6188.

6 G. Cera, M. Bazzoni, A. Arduini and A. Secchi, *Org. Lett.*, 2020, **22**, 3702.

7 G. Cera, D. Balestri, M. Bazzoni, L. Marchiò, A. Secchi and A. Arduini, *Org. Biomol. Chem.*, 2020, **18**, 6241.

8 S. Shinkai, S. Mori, H. Koreishi, T. Tsubaki and O. Manabe, *J. Am. Chem. Soc.*, 1986, **108**, 2409.

9 (*a*) S. Sayin and M. Yilmaz, *Tetrahedron*, 2014, **37**, 6669; (*b*) Y. Xie, L. Mao and L. Li, *J. Chem. Res.*, 2013, **37**, 476; (*c*) Y.-L. Liu, L. Liu, Y.-L. Wang, Y.-C. Han, D. Wang and Y.-J. Chen, *Green Chem.*, 2008, **10**, 635; (*d*) S. Shimizu, N. Shimada and Y. Sasaki, *Green Chem.*, 2006, **8**, 608.

10 (*a*) T. Siodła, W. P. Oziminski, M. Hoffmann, H. Koronia and T. M. Krygowski, *J. Org. Chem.*, 2014, **79**, 7321; (*b*) B. A. Shainyan and L. L. Tolstikova, *Chem. Rev.*, 2013, **113**, 699; J. E. True, T. D. Thomas, R. W. Winter and G. L. Gard, *Inorg. Chem.*, 2003, **42**, 4437.

11 (*a*) S. Zhang, D. Lebœuf and J. Moran, *Chem. – Eur. J.*, 2020, **26**, 9883; (*b*) K. M. Diemoz and A. K. Franz, *J. Org. Chem.*, 2019, **84**, 1126.

12 (*a*) M. A. Beckett, D. S. Brassington, S. J. Coles and M. B. Hursthouse, *Inorg. Chem. Commun.*, 2000, **3**, 530; (*b*) M. A. Beckett, G. C. Strickland, J. R. Holland and K. A. Sukumar Varma, *Polymer*, 1996, **37**, 4629; (*c*) V. Gutmann, *Coord. Chem. Rev.*, 1976, **18**, 225.

13 See ESI† for more details.

14 For selected examples of ion-pair induced conformational control, see: (*a*) S. K. Kim, V. M. Lynch, B. P. Hay, J. S. Kim and J. L. Sessler, *Chem. Sci.*, 2015, **6**, 1404; (*b*) S. Moerkerke, J. Wouters and I. Jabin, *J. Org. Chem.*, 2015, **80**, 8720. For a recent review, see: (*c*) M. Wenzel, J. R. Hiscock and P. A. Gale, *Chem. Soc. Rev.*, 2012, **41**, 480.

15 For recent examples of sulfonamide catalysts, see: (*a*) M. Yuan, I. I. Mbaezue, Z. Zhou, F. Topic and Y. S. Tsantrizos, *Org. Biomol. Chem.*, 2019, **17**, 8690; (*b*) H. Tanaka, K. Sakai, A. Kawamura, K. Oisaki and M. Kanai, *Chem. Commun.*, 2018, **54**, 3215; S. Takata, Y. Endo, M. Shaid Ullah and S. Itsuno, *RSC Adv.*, 2016, **6**, 72300; (*c*) T. Kano, R. Sakamoto, M. Akakura and K. Maruoka, *J. Am. Chem. Soc.*, 2012, **134**, 7516.

16 (*a*) C. Deraedt and D. Astruc, *Coord. Chem. Rev.*, 2016, **324**, 106; (*b*) Z. Dong, Q. Luo and J. Liu, *Chem. Soc. Rev.*, 2012, **41**, 7890; (*c*) L. Marchetti and M. Levine, *ACS Catal.*, 2011, **1**, 1090.

17 For recent reviews, see: (*a*) Y. Huang, J. Ren and X. Qu, *Chem. Rev.*, 2019, **119**, 4357; (*b*) J. Shi, Y. Wu, S. Zhang, Y. Tian, D. Yang and Z. Jiang, *Chem. Soc. Rev.*, 2018, **47**, 4295.

18 For recent supramolecular Michael additions, see: (*a*) P. La Manna, M. De Rosa, C. Talotta, A. Rescifina, G. Floresta, A. Soriente, C. Gaeta and P. Neri, *Angew. Chem.*, 2020, **59**, 811; (*b*) S. Gambaro, M. De Rosa, A. Soriente, C. Talotta, G. Floresta, A. Rescifina, C. Gaeta and P. Neri, *Org. Chem. Front.*, 2019, **6**, 2339; (*c*) U. Vural, M. Durmaz and A. Sirit, *Org. Chem. Front.*, 2016, **3**, 730.

19 (*a*) P. W. N. M. van Leeuwen and M. Raynal, in *Supramolecular Chemistry in Water*, ed. S. Kubik, Wiley–VCH Verlag GmbH & Co. KGaA, 2019, vol. 14, pp. 525. For a recent review on supramolecular organocatalysis in water, see: (*b*) M. De Rosa, P. La Manna, C. Talotta, A. Soriente, C. Gaeta and P. Neri, *Front. Chem.*, 2018, **6**, 84.

20 (*a*) S. Narayan, J. Muldoon, M. G. Finn, V. V. Fokin, H. C. Kolb and K. B. Sharpless, *Angew. Chem., Int. Ed.*, 2005, **44**, 3275; (*b*) R. N. Butler and A. G. Coyne, *Chem. Rev.*, 2010, **110**, 6302; (*c*) R. Breslow, *Acc. Chem. Res.*, 1991, **24**, 159.

21 For a seminal work, see; D. M. Rudkevich, *Chem. – Eur. J.*, 2000, **6**, 2679.

22 (*a*) X.-W. Dong, T. Liu, Y.-Z. Hu, X.-Y. Liu and C.-M. Che, *Chem. Commun.*, 2013, **49**, 7681; (*b*) M. Bandini and A. Eichholzer, *Angew. Chem., Int. Ed.*, 2009, **48**, 9608.

23 M. De Rosa and A. Soriente, *Tetrahedron*, 2010, **66**, 2981.
24 (*a*) A. Shokri, X.-B. Wang and S. R. Kass, *J. Am. Chem. Soc.*, 2013, **135**, 9525; (*b*) A. Shokri, A. Abedin, A. Fattahi and S. R. Kass, *J. Am. Chem. Soc.*, 2012, **134**, 10646.
25 R.-J. Tang, T. Milcent and B. Crousse, *RSC Adv.*, 2018, **8**, 10314 and references therein.
26 A. V. Kumar and R. Rao, *Tetrahedron Lett.*, 2011, **52**, 5188.
27 G. Bartoli, M. Bosco, S. Giuli, A. Giuliani, L. Lucarelli, E. Marcantoni, L. Sambri and E. Torregiani, *J. Org. Chem.*, 2005, **70**, 1941.
28 S. Yadav, M. Srivastava, P. Rai, B. P. Tripathi, A. Mishra, J. Singh and J. Singh, *New J. Chem.*, 2016, **40**, 9694 and references therein.
29 W.-G. Huang, H.-S. Wang, G.-B. Huang, Y.-M. Wu and Y.-M. Pan, *Eur. J. Org. Chem.*, 2012, 5839.